American Journal of Analytical Chemistry, 2015, 6, 118-126
Published Online January 2015 in SciRes. http://www.scirp.org/journal/ajac
http://dx.doi.org/10.4236/ajac.2015.62011

Kinetics and Vapor Pressure Studies of bis(*N*-alkyl-2-hydroxonapthaldimine)nickel (II) (*N*-R = methyl to pentyl) Complexes

Maria Francis George Johnson[1], Thevabakthi Siluvai Muthu Arul Jeevan[2*], Sebastian Arockiasamy[3], Karachalacheruvu Seetharamaiah Nagaraja[1]

[1]Department of Chemistry, Loyola Institute of Frontier Energy (LIFE), Loyola College, Chennai, India
[2]Department of Chemistry, College of Natural and Computational Sciences, University of Gondar, Gondar, Ethiopia
[3]Department of Chemistry, School of Advanced Sciences (SAS), VIT University Chennai Campus, Chennai, India
Email: *jejeevan@gmail.com

Received 29 December 2014; accepted 16 January 2015; published 20 January 2015

Abstract

The complexes of bis[*N*-alkyl-2-hydroxonapthaldimine]nickel(II) (*N*-alkyl = methyl, ethyl, propyl, butyl or pentyl) were synthesized and their volatilization in N_2 atmosphere was demonstrated by the TG-based transpiration technique. The equilibrium vapor pressure of the complexes over a temperature span of 470 - 590 K was determined by adapting a horizontal dual arm single furnace thermoanalyser as a transpiration apparatus. It yielded $\Delta_{vap}H^{o}$ as 153.1 (±1.9), 122.9 (±0.3), 147.6 (±10.7), 151.8 (±10.9) and 114.7 (±5.3) k·Jmol^{-1} respectively. The entropies of vaporization $\left(\Delta_{vap}S^{o}\right)$ for these complexes as calculated from the intercept of the linear fit expressions were found to be 319.7 (±3.9), 229.9 (±5.8), 317.8 (±17.2), 319.7 (±19.1) and 254.6 (±9.6) Jmol^{-1}·K^{-1} respectively. The non-isothermal vaporization activation energy was determined from Arrhenius and Coats-Redfern methods.

Keywords

Volatile Nickel Complexes, Thermal Properties, Vapor Pressure, Transpiration Technique, Enthalpy and Entropy of Vaporization, Vaporization Kinetics

1. Introduction

Success of the metallo-organic chemical vapor deposition (MOCVD) technique for preparing thin films rests

*Corresponding author.

How to cite this paper: Johnson, M.F.G., *et al.* (2015) Kinetics and Vapor Pressure Studies of bis(*N*-alkyl-2-hydroxonapthaldimine)nickel(II) (*N*-R = methyl to pentyl) Complexes. *American Journal of Analytical Chemistry*, **6**, 118-126.
http://dx.doi.org/10.4236/ajac.2015.62011

mainly on the availability of completely volatile precursors. Therefore, development of stable, non-toxic and completely volatile solid metallo-organic precursors for use in CVD of metallic nickel has attracted intensive research [1]-[7]. Many publications warned the use of highly toxic $Ni(CO)_4$ as a precursor [8] [9], which was first used by Mond in 1885. Other precursors used in MOCVD of Ni films are $Ni(acac)_2en$ [1], $Ni(tfacim)_2$ (tfacim = triflouroacetylacetone-imine) [3] [4], $Ni(L)_2$ [L= dimethylglyoxime [10], diethylglyoxime, dipropylglyoxime [6]], $Ni(\eta^5\text{-}C_5H_5)_2$ [7], $Ni(L)_2$ [L = acetylacetone (acac) [11], hexafluoroacetylacetone (hfac) [12] and tetramethylheptanedione (tmhd) [13]]. $Ni(tmhd)_2$ [14] and Ni[$(acac)_2en$] [1] met the requirements of an ideal precursors in CVD applications. It is essential to synthesize new precursors with mixed O and N environment around Ni employing aromatic ligands for better volatility. This paper describes the synthesis and characterization of nickel complexes by using Schiff base ligands. These complexes are characterized by elemental analyses, FT-IR, FABMS, TG/DTA, vaporization kinetics and vapor pressure measurement by the TG-based transpiration technique.

2. Experimental

$NiCl_2{\cdot}6H_2O$, 2-hydroxynaphthal (Aldrich), methylamine, ethylamine, propylamine, butylamine, pentylamine (Loba Chemie, India), liquor ammonia and methanol (S. D. Fine, India) were used as procured.

2.1. Synthesis of the Complexes

2.1.1. Synthesis of bis(2-hydroxonapthaldehydato)nickel(II) [Ni(2-hydroxynapthal)2]

$NiCl_2{\cdot}6H_2O$ (9.48 g) was dissolved in water (20 cm^3) to which 2-hydroxynaphthal (10 cm^3) was added drop-wise under constant stirring. To this reaction mixture, liquor ammonia (12 cm^3) was added drop-wise by continuously monitoring the formation of a greenish yellow precipitate. This precipitate was digested at 333 K over a water bath for 0.5 h, which was filtered, washed with ethanol and dried under vacuum [15]. Yield: 76%.

2.1.2. Syntheses of bis(*N*-alkyl-2-hydroxonapthaldimine)nickel(II) complexes [*N*-alkyl = methyl to pentyl]

The syntheses of bis(*N*-alkyl-2-hydroxonapthaldimine)nickel(II), where *N*-alkyl = methyl to pentyl complexes were carried out by treating the appropriate primary amines with the hot alcoholic suspension of Ni(2-hydroxonapthal)$_2$. The resulting olive green solution was refluxed for about 0.5 h and the crystals formed were filtered, washed with ethanol and dried under vacuum. The compound was recrystallized from methanol. Yield: 56% - 82%.

2.2. Characterization

The C, H and N analyses were performed on a CARBO-ERBA-11008 rapid elemental analyzer. IR spectra were recorded as KBr pellets on a Perkin-Elmer FT-IR spectrometer (RX1, FT-IR) in the region of 4000 - 450 cm^{-1}. Fast atom bombardment mass spectra (FABMS) of the nickel complexes were recorded by employing a JEOL SX 102/DA-6000 spectrometer using argon as the FAB gas with an accelerating voltage of 10 kV and the spectra were recorded at room temperature. M-nitrobenzyl alcohol (NBA) was used as the matrix unless specified otherwise. The thermal analyses were carried out using Perkin-Elmer, Pyris Diamond TG/DTA at a linear heating rate of 0.17 Ks^{-1}. High purity nitrogen (purity > 99.99%) dried by passing through refrigerated molecular sieves (Linde 4A) was used as the purge gas at a flow rate of 12 $dm^3{\cdot}h^{-1}$.

2.3. Vapor Pressure Measurement Studies

A horizontal thermal analyzer was adapted as a transpiration setup for vapor pressure measurements. The configuration of the horizontal dual arm with a single narrow furnace chamber minimizes errors arising from convection, buoyancy, thermo molecular and electrostatic charge effects. The arms of the thermo balance served as the temperature-cum-DTA sensors.

The block diagram of the thermal analyzer, modification for its functioning in the transpiration mode, including precise flow calibration for the carrier gas using a capillary glass flow meter and corrections for apparent weight losses in isothermal mode were the same as reported [15] [16]. The choice of 6 $dm^3{\cdot}h^{-1}$ for N_2 gas was made for the isothermal equilibrium vaporization on the basis of the existence of a plateau in the plot of the equilibrium

vapor pressure (p_e) against the flow rate. The vapor pressure measurements were carried out by rapid heating 0.17 Ks^{-1} and after allowing for temperature stabilization, subsequent changes in isothermal steps were done at a heating rate of 0.03 Ks^{-1}. It turned out that the vapor pressure (p_e) derived from the TG-based transpiration method was reliable to 10% accuracy [15] [16].

2.4. Vaporization Kinetics

Experiments were performed under non-isothermal conditions at a programmed linear heating rate of 10˚C·min^{-1} for methyl to pentyl homologues. Among the various methods for the kinetics evaluation of TG weight loss data, Arrhenius method was followed in the present investigation to study the vaporization kinetics.

3. Results and Discussion

3.1. Thermal Analyses

The elemental analyses and their composition are presented in **Table 1**. The melting point endotherms (**Figure 1**) were calculated accurately using the built-in Pyris software and the values 280˚C, 271˚C, 205˚C, 176˚C and 175˚C for methyl to pentyl homologues respectively which exhibited a decreasing trend with increasing length of the alkyl chain. The non-isothermal TG curves (**Figure 2**) of bis(2-hydroxonapthaldehydato)nickel(II) indicated a 37.8% residue at 700 K making it unsuitable for CVD applications. The TG curves of bis(*N*-alkyl-2-hydroxonapthaldimine)nickel(II) homologues (where *N*-alkyl = methyl to pentyl) showed a single step weight loss commencing from 700 K, leading to a negligible amount of residue qualifying themselves as precursors for CVD.

3.2. Spectral Characterization

The relevant frequencies such as $\nu_{(C=N)}$, $\nu_{(C=C)}$, $\nu_{C-O(phenolic)}$ $\nu_{(Ni-N)}$ and $\nu_{(Ni-O)}$ (**Table 2**) support the structure. The FABMS patterns (**Table 3**) of bis[*N*-alkyl-2-hydroxonapthaldimine)]nickel(II) (where *N*-alkyl = methyl to pentyl) complexes revealed the molecular masses (M) of the complexes and their fragmentation pattern. The values of molecular ion peaks were observed at m/z (Da) = 430, 454, 483, 510 and 539 respectively, for methyl to pentyl homologues as clusters due to the isotopic abundances of natural nickel (^{58}Ni: 67.76%, ^{60}Ni: 26.16%, ^{61}Ni: 1.25%, ^{62}Ni: 3.66%, ^{64}Ni: 1.16%).

3.3. Vapor Pressure Measurements

Effective control of the process of any type of CVD and to monitor the composition, thickness and microstructure of thin films, relevant information on precursor chemistry, possible fragmentation pattern by the decomposition of precursors and vapor pressures are needed. Therefore vapor pressure measurement was deemed as essential for these complexes to be used for MOCVD.

If W is the mass loss of the sample (**Table 4**) at the isothermal temperature caused by the flow of V_c dm^3 of the carrier gas (measured at $T_c = 298$ K), the vapor pressure p_e could be calculated using Dalton's law of partial pressure for ideal gas mixtures as

$$(p_e)_T = WRT/MV_c \tag{1}$$

where M is the molar mass of the complexes, T_c and V_c are the temperature and volume of the carrier gas respectively. The molecular mass of the congruently vaporizing species was obtained from FABMS. The observed mass loss and the calculated p_e (using Equation (1)) (**Table 4**) and $\log(p_e/MP_a)$ versus 1000/T (K) are shown in **Figure 3**. The values of slope (B) and intercept (A) of the Clausius-Clapeyron equation obtained from the plot for the nickel homologues (**Table 5**) along with the values of enthalpy of vaporization $(\Delta_{vap}H°)$ and entropy of vaporization $(\Delta_{vap}S°)$ are given.

$$\log\{p_e/MP_a\} = A - B\left/\left[\frac{10^5}{T}\right]\right. \tag{2}$$

Table 1. Elemental analyses and melting points of bis(*N*-alkyl-2-hydroxonapthaldimine)nickel(II) complexes.

S. No.	Complexes	*N*-R	M.p	Elemental Analyses		
			(˚C)	C	H	N
1	$[Ni(C_{24}H_{22}N_2O_2)]$	Methyl	280.5	67.16 (67.82)	5.16 (4.88)	6.52 (6.73)
2	$[Ni(C_{26}H_{26}N_2O_2)]$	Ethyl	270.81	68.30 (68.33)	5.73 (5.40)	6.12 (6.47)
3	$[Ni(C_{28}H_{30}N_2O_2)]$	Propyl	205.5	69.30 (69.92)	6.23 (6.08)	5.77 (6.03)
4	$[Ni(C_{30}H_{34}N_2O_2)]$	Butyl	176.92	70.19 (70.23)	6.67 (6.99)	5.45 (5.44)
5	$[Ni(C_{32}H_{38}N_2O_2)]$	Pentyl	175.13	70.99 (71.34)	7.07 (6.91)	5.17 (5.10)

Table 2. Relevant IR frequencies of bis(*N*-alkyl-2-hydroxonapthaldimine)nickel(II).

S. No.	*N*-R	Groups				
		$\nu_{(C=N)}$	$\nu_{(C=C)}$	$\nu_{C-O(phenolic)}$	$\nu_{(Ni-N)}$	$\nu_{(Ni-O)}$
1	Methyl	1617	1540	1326	541	488
2	Ethyl	1618	1543	1326	540	469
3	Propyl	1613	1552	1332	533	461
4	Butyl	1612	1564	1329	532	475
5	Pentyl	1615	1542	1332	549	496

Table 3. Assignment of peaks in FAB mass spectra of bis(*N*-alkyl-(2-hydroxonapthal)nickel(II) complexes; *N*-alkyl = methyl (a) to pentyl (e) respectively.

Ions	a		b		c		d		e	
	m/z	% Rel. int	*m/z*	% Rel. int	*m/z*	% Rel. int	*m/z*	% Rel. int	*m/z*	% Rel. int
$[NiL_{2+1/3}]^+$	492	22	516	3	539	3	568	17	598	35
$[NiL_2]^+$	430	100	454	100	483	100	510	100	539	100
$[NiL]^+$	244	13	255	25	269	22	283	46	298	12
$[L]^+$	186	53	199	66	212	16	226	22	240	26
$[NiL_2 - C_{10}H_8O]^+$	307	42	327	13	363	6	x	x	x	x

Table 4. Mass loss (for 60 min) and for equilibrium solid vaporization of bis(*N*-alkyl-2-hydroxonapthaldimine)nickel(II) homologues by TG-based transpiration method.

S. No.	*T* (K)	Mass loss (mg)	p_e/MPa	S. No.	*T* (K)	Mass loss (mg)	pe/MPa
	Methyl			3	570	1.405	1203
1	571	0.572	555	4	580	2.091	1790
2	576	0.687	665		**Butyl**		
3	582	0.904	876	1	549	0.207	168
4	587	1.206	1168	2	559	0.394	319
	Ethyl			3	570	0.808	654
1	556	0.414	376	4	580	1.202	973
2	569	0.785	713		**Pentyl**		
3	580	1.222	1111	1	549	0.335	257
4	591	2.091	1757	2	560	0.503	386
	Propyl			3	570	0.785	603
1	549	0.375	321	4	580	1.293	992
2	560	0.76	651				

Table 5. Clausius-Clapeyron parameters for bis(*N*-alkyl-2-hydroxonapthaldimine)nickel(II).

S. No.	*N*-R	$\log(p_e/MP_a) = A - B/[1000/T(\mathrm{K})]$			$\Delta_{vap}H^o$	$\Delta_{vap}S^o$
		A	B	Temperature range (K)	$KJmol^{-1}$	$JK^{-1}mol^{-1}$
1	Methyl	16.7 (±0.2)	7994.7 (±99.2)	571 - 587	153.1 (±1.9)	319.7 (±3.9)
2	Ethyl	14.1 (±0.3)	6423.7 (±20.0)	556 - 591	122.9 (±0.3)	229.9 (±5.8)
3	Propyl	16.6 (±0.9)	7706.4 (±563.9)	549 - 580	147.6 (±10.7)	317.8 (±17.2)
4	Butyl	16.7 (±1.0)	7929.4 (±573.8)	549 - 580	151.8 (±10.9)	319.7 (±19.1)
5	Pentyl	13.3 (±0.5)	5989.7 (±276.2)	549 - 580	114.7 (±5.3)	254.6 (±9.6)

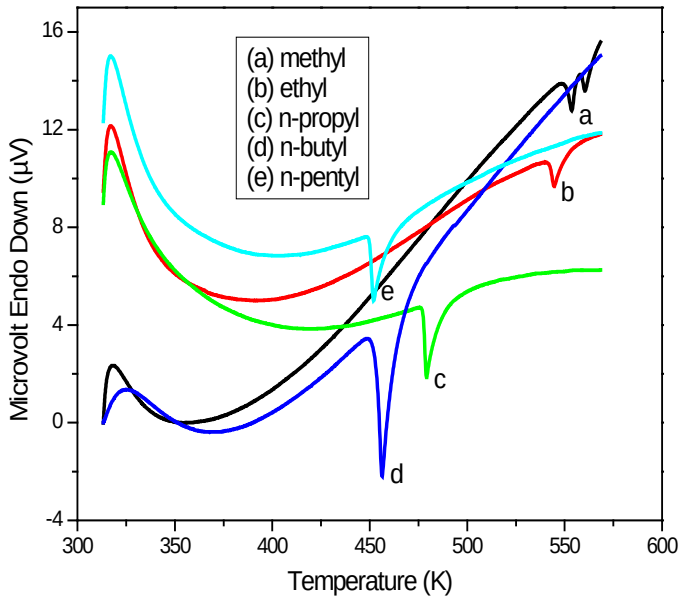

Figure 1. DTA traces of bis(*N*-alkyl-2-hydroxonapthaldimine)nickel(II).

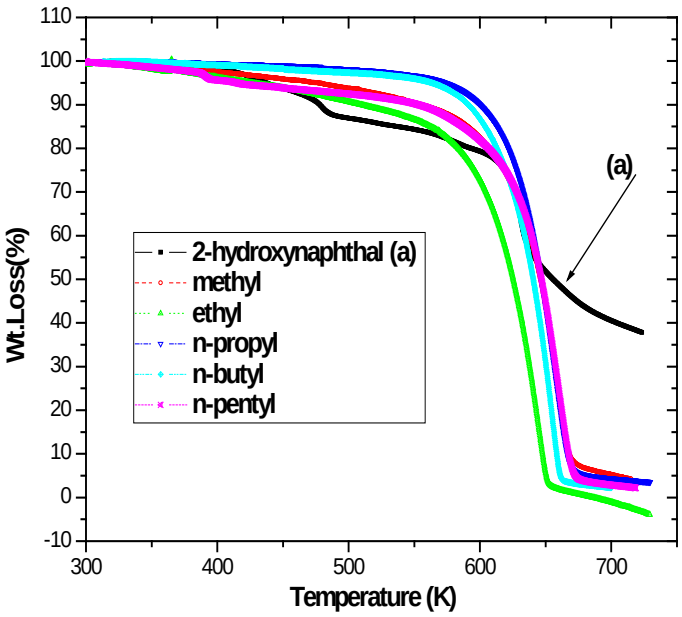

Figure 2. Non-isothermal TG curves of nickel complexes.

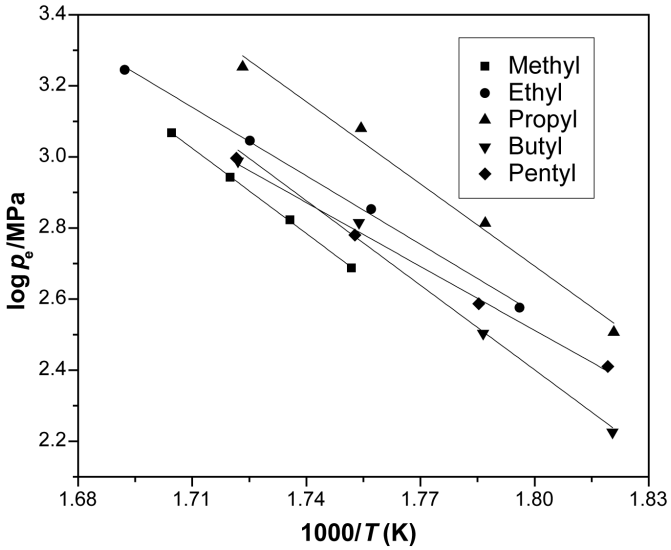

Figure 3. Clausius-Clapeyron plots for bis(*N*-alkyl-2-hydroxonapthaldimine)nickel(II) homologues.

Enthalpy of vaporization is obtained by multiplying the slope B in Equation (2) with −2.303 R. The least-square expressions from the plots are included in **Table 5** along with the temperature ranges of their experimental measurements employing the TG-based transpiration technique. The values as calculated from the slope of the curve were found to be 153.1 (±1.9), 122.9 (±0.3), 147.6 (±10.7), 151.8 (±10.9) and 114.7 (±5.3) k·Jmol^{-1} respectively. The entropies of vaporization $\left(\Delta_{\text{vap}}S°\right)$ for these complexes as calculated from the intercept of the linear fit expression were found to be 319.7 (±3.9), 229.9 (±5.8), 317.8 (±17.2), 319.7 (±19.1) and 254.6 (±9.6) Jmol^{-1}·K^{-1}. The vapor pressure of the complexes will be helpful for fixing the metal organic chemical vapor deposition (MOCVD) process parameters for getting the desired phase and rate of deposition of nickel and composite materials.

3.4. Determination of Activation Energy $\left(E_a\right)$

The rate constant k for the vaporization enthalpy of the complexes was determined in the temperature range of 400 - 680 K for every 10% weight loss of the complex. The expression (3) for k is given by

$$k = \mathrm{d}\alpha/\mathrm{d}t \tag{3}$$

where $\mathrm{d}\alpha/\mathrm{d}t$ is the derivative of the fraction vaporized with respect to time and k is the rate constant of vaporization. For every 10% weight loss, α was calculated by the expression (4) as

$$\alpha = \frac{\%W_i - \%W_t}{\%W_i - \%W_f} \tag{4}$$

where $\%W_t$ is the per cent weight at any time t and $\%W_i$ and $\%W_f$ respectively, are the initial and final percent sample weights [17]. The Arrhenius expression (5) is

$$k = A\mathrm{e}^{\frac{-E}{RT}} \tag{5}$$

And the plot of $\ln k$ versus 1000/T (K) (**Figure 4**) is found to be linear. From the slope, the activation energy $\left(E_a\right)$ for the vaporization of the complexes was calculated. The activation energy values were found to be 106 ± 4, 111 ± 6, 114 ± 7, 115 ± 7 and 121 ± 4 k·Jmol^{-1} respectively for methyl to pentyl homologues.

The kinetics of the complexes was followed by employing the Coats-Redfern approximation which gives the expression (6).

$$\ln\left[\frac{g(\alpha)}{T^2}\right] = \left[\frac{AR}{\beta E}\left(1 - \frac{2RT}{E}\right)\right]\frac{E}{RT} \tag{6}$$

A plot of $\ln\left[g(\alpha)=T^2\right]$ versus 1000/T (K) gives (**Figure 5**) a straight line when the correct $g(\alpha)$ function is used in the equation. The $g(\alpha)$ function describes the mechanism of the reaction [18]. Straight lines with high-correlation coefficient and low standard deviation were selected to represent the possible controlling mechanism. The corresponding kinetic parameters were then calculated and are shown in **Table 6**. The best fit for the methyl complex is obtained using A3 Avrami-Erofe'ev Equation (3). For the ethyl and pentyl complexes, best fit was obtained with R2, contracting area model. For the propyl and butyl complexes, best fit was obtained with A2, two dimensional Avrami-Erofe'ev Equations (2) model. The activation energy values were found to be 112 (±5), 115 (±5), 105 (±6), 108 (±10) and 126 (±5) k·Jmol^{-1} respectively for methyl to pentyl homologues. Analysis of these data show that the activation energies which are in good agreement with that obtained using Arrhenius's method.

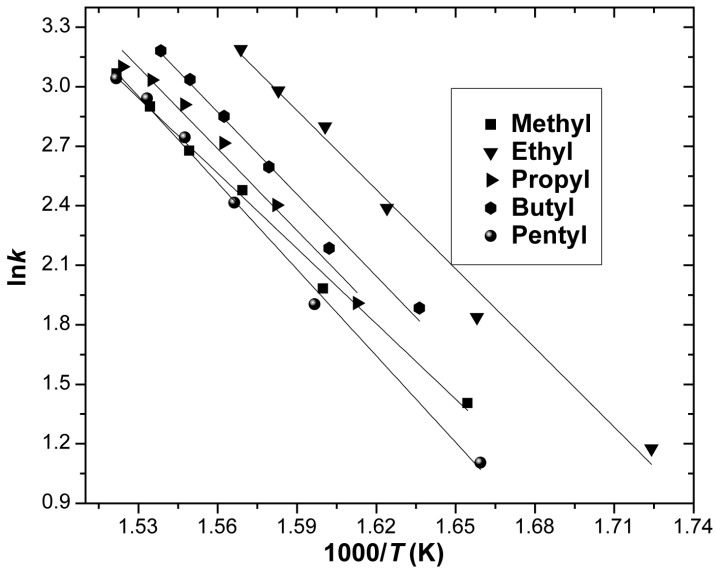

Figure 4. Arrhenius plots of bis(*N*-alkyl-2-hydroxonapthaldimine)nickel(II).

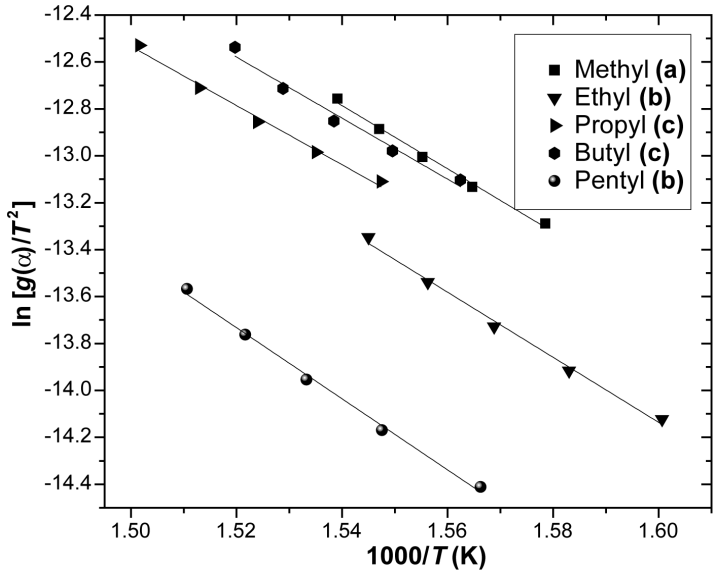

Figure 5. Plots of $\ln\left[g(\alpha)/T^2\right]$ versus 1000/T (K); where $g(\alpha)=\left[-\ln(1-\alpha)\right]^{1/3}$ (a); $\left[1-(1-\alpha)\right]^{1/2}$ (b); and $\left[-\ln(1-\alpha)\right]^{1/2}$ (c).

Table 6. Activation energies obtained using the Coats-Redfern method for several solid state processes at heating rate of 10˚C·min^{-1} for methyl to pentyl.

Model	Methyl		Ethyl		Propyl		Butyl		Pentyl	
	E_a (k·Jmol^{-1})	R	E_a (k·Jmol^{-1})	R	E_a (k·Jmol^{-1})	R	E_a (k·Jmol^{-1})	R	E_a (k·Jmol^{-1})	R
A2	173 (±7)	0.9973	77 (±7)	0.989	**105 (±6)**	**0.9957**	**108 (±10)**	**0.9899**	84 (±6)	0.9888
A3	**112 (±5)**	0.9972	48 (±4)	0.9874	66 (±4)	**0.9952**	69 (±6)	0.9889	53 (±4)	0.9873
A4	81 (±4)	0.997	33 (±3)	0.9854	47 (±3)	0.9947	49 (±4)	0.9877	37 (±3)	0.9855
R2	288 (±3)	0.9998	**115 (±5)**	**0.9973**	149 (±1)	0.9999	157 (±6)	0.9998	**126 (±5)**	**0.9979**
R3	310 (±6)	0.9993	130 (±7)	0.9951	171 (±4)	0.9992	178 (±9)	0.9959	146 (±7)	0.9957
D1	472 (±14)	0.9987	168 (±1)	0.9999	206 (±16)	0.9971	221 (±2)	0.9998	197 (±3)	0.9995
D2	542 (±7)	0.9997	210 (±5)	0.999	265 (±4)	0.9996	281 (±5)	0.9995	241 (±4)	0.9993
D3	630 (±13)	0.9993	271 (±15)	0.9956	352 (±8)	0.9993	367 (±19)	0.9962	302 (±1)	0.9959
D4	571 (±5)	0.9998	230 (±8)	0.998	293 (±1)	0.9999	309 (±9)	0.9987	261 (±7)	0.9985
F1	357 (±15)	0.9966	164 (±13)	0.9903	221 (±11)	0.9961	227 (±18)	0.9908	180 (±13)	0.99
F2	291 (±58)	0.9448	209 (±40)	0.9496	318 (±53)	0.9611	302 (±59)	0.9488	210 (±41)	0.9304

4. Conclusion

The thermodynamic and kinetic decomposition of bis(*N*-alkyl-2-hydroxonapthaldimine)nickel(II) (*N*-alkyl = methyl, ethyl, propyl, butyl or pentyl) complexes were carried out. The molecular masses of the homologous series of the nickel complexes were obtained from FABMS. The TG-based transpiration technique was used to evaluate the vapor pressure data of bis(*N*-alkyl-2-hydroxonapthaldimine)nickel(II) homologues. The standard enthalpies of vaporization and entropies of vaporization of the complexes have been evaluated. The non-isothermal vaporization activation energy values were determined by Arrhenius and Coats-Redfern methods.

Acknowledgements

This work received financial support from the Department of Science and Technology (DST), India, through Grant No. SR/S3/ME/03/2005-SERC-Engg. The authors thank the Central Drug Research Institute, Lucknow, for recording the mass spectra and C, H and N analyses.

References

[1] Premkumar, P.A., Dasgupta, A., Kuppusami, P., Parameswaran, P., Mallika, C., Nagaraja, K.S. and Raghunathan, V.S. (2006) Synthesis and Characterization of Ni and Ni/CrN Nanocomposite Coatings by Plasma Assisted Metal-Organic CVD. *Chemical Vapor Deposition*, **12**, 39-45. http://dx.doi.org/10.1002/cvde.200506415

[2] Hunde, E.T. and Watkins, J.J. (2004) Reactive Deposition of Cobalt and Nickel Films from Their Metallocenes in Supercritical Carbon Dioxide Solution. *Chemistry of Materials*, **16**, 498-503. http://dx.doi.org/10.1021/cm034433n

[3] Bakovets, V.V., Mitkin, V.N. and Gelfond, N.V. (2005) Mechanism of Ni Film CVD with a Ni(Ktfaa)$_2$ Precursor on a Silicon Substrate. *Chemical Vapor Deposition*, **11**, 368-374. http://dx.doi.org/10.1002/cvde.200506376

[4] Bakovets, V.V., Mitkin, V.N. and Gelfond, N.V. (2005) Mechanism of Ni Film CVD with a Ni(ktfaa)$_2$ Precursor on a Copper Substrate. *Chemical Vapor Deposition*, **11**, 112-117. http://dx.doi.org/10.1002/cvde.200406317

[5] Zhou, M., Lin, W.Y., de Tacconi, N.R. and Rajeshwar, K. (1996) Metal/Semiconductor Electrocomposite Photoelectrodes: Behavior of Ni/TiO$_2$ Photoanodes and Comparison of Photoactivity of Anatase and Rutile Modifications. *Journal of Electroanalytical Chemistry*, **402**, 221-224. http://dx.doi.org/10.1016/0022-0728(95)04368-3

[6] Brissonneau, L. and Vahlas, C. (1999) MOCVD-Processed Ni Films from Nickelocene. Part I: Growth Rate and Morphology. *Chemical Vapor Deposition*, **5**, 135-142. http://dx.doi.org/10.1002/(SICI)1521-3862(199908)5:4<135::AID-CVDE135>3.0.CO;2-1

[7] Stauf, G., Driscoll, D., Dowben, P., Barfuss, S. and Grade, M. (1987) Iron and Nickel Thin Film Deposition via Metallocene Decomposition. *Thin Solid Films*, **153**, 421-430. http://dx.doi.org/10.1016/0040-6090(87)90202-1

[8] Kang, J.K. and Ree, S.W. (2000) Metalorganic Chemical Vapor Deposition of Nickel Films from Ni(C$_5$H$_5$)$_2$/H$_2$. *Jour-*

nal of Materials Research, **15**, 1828-1833. http://dx.doi.org/10.1557/JMR.2000.0264

[9] Maruyama, T. and Tago, T. (1993) Nickel Thin Films Prepared by Chemical Vapor Deposition from Nickel Acetylacetonate. *Journal of Materials Science*, **28**, 5345-5348. http://dx.doi.org/10.1007/BF00570088

[10] Becht, M., Gallus, J., Hunziker, M., Atamny, F. and Dahmen, K.H. (1995) Nickel Thin Films Grown by MOCVD Using $Ni(dmg)_2$ as Precursor. *Journal de Physique IV*, **C5**, 465-472.

[11] Hemert, R.V., Spenlove, L. and Sievers, S. (1965) Vapor Deposition of Metals by Hydrogen Reduction of Metal Chelates. *Journal of the Electrochemical Society*, **112**, 1123-1126. http://dx.doi.org/10.1149/1.2423376

[12] Lane, P.A., Crosbie, M.J., Wright, P.J., Donohue, P.P., Hirst, P.J., Reeves, C.L., Anthony, C.J., Jones, A.C., Todd, M.A. and Williams, D.J. (2003) The Metal-Organic Chemical Vapor Deposition of Lanthanum Nickelate Electrodes for Use in Ferroelectric Devices. *Chemical Vapor Deposition*, **9**, 87-92. http://dx.doi.org/10.1002/cvde.200390007

[13] Anthony, C.J. (1998) MOCVD of Electroceramic Oxides: A Precursor Manufacturer's Perspective. *Chemical Vapor Deposition*, **4**, 169-179. http://dx.doi.org/10.1002/(SICI)1521-3862(199810)04:05<169::AID-CVDE169>3.3.CO;2-Y

[14] Wood, J.L. and Jones, M. (1963) Heats of Formation and Coordinate Bond Energies of Some Nickel(II) Chelates. *Journal of Physical Chemistry*, **67**, 1049-1051. http://dx.doi.org/10.1021/j100799a024

[15] Pankajavalli, R., Mallika, C., Sreedharan, O.M., Premila, M. and Gopalan, P. (1998) Vapor Pressure of C_{60} by a Transpiration Method Using a Horizontal Thermobalance. *Thermochimica Acta*, **316**, 101-108. http://dx.doi.org/10.1016/S0040-6031(98)00304-9

[16] Arockiasamy, S., Sreetharan, O.M., Mallika, C., Raghunathan, V.S. and Nagaraja, K.S. (2007) Development, Characterisation and Rapid Evaluation of Standard Enthalpies of Vaporisation and Fusion of Volatile Bis(N-R-Salicylaldimine) Nickel(II) (n-R = Methyl to Pentyl) Complexes for Its MOCVD Applications. *Chemical Engineering Science*, **62**, 1703-1711. http://dx.doi.org/10.1016/j.ces.2006.12.001

[17] Burnham, L., Dollimore, D. and Alexander, K. (2001) Calculation of the Vapor Pressure-Temperature Relationship Using Thermogravimetry for the Drug Allopurinol. *Thermochimica Acta*, **367**, 15-22. http://dx.doi.org/10.1016/S0040-6031(00)00652-3

[18] Joseph, K., Sridharan, R. and Gnanasekaran, T. (2000) Kinetics of Thermal Decomposition of $Th(C_2O_4)_2 \cdot 6H_2O$. *Journal of Nuclear Materials*, **281**, 129-139. http://dx.doi.org/10.1016/S0022-3115(00)00241-5